

Taking Advantage of Disorder: Small-Molecule Organic Glasses for Radiation Detection and Particle Discrimination

Joseph S. Carlson, Peter Marleau, Ryan A. Zarkesh, Patrick L. Feng*

Sandia National Laboratories, 7011 East Ave., Livermore, CA 94550

ABSTRACT: A series of fluorescent silyl-fluorene molecules were synthesized and studied with respect to their photo-physical properties and response toward ionizing neutron and gamma-ray radiation. Several of the prepared compounds were found to form transparent bulk organic glasses capable of providing fluorescence quantum yields and radiation detection properties exceeding the highest-performing benchmark materials such as solution-grown *trans*-stilbene crystals. Secondary dopants comprising singlet fluorophores or iridium organometallic compounds provided improved detection efficiency, as evaluated by light yield and neutron/gamma particle discrimination measurements. Optimized singlet and triplet doping levels were determined to be 0.05 wt. % 1,4-*bis*(2-methylstyryl)benzene (*bis*-MSB) singlet fluorophore and 0.28 wt. % Ir³⁺, which indicates efficient Förster Resonance Energy Transfer (FRET) and host-guest triplet-harvesting interactions, respectively. Co-melts based on blends of two different glass-forming compounds were prepared with the goal of enhancing the stability of the amorphous state. Accelerated aging experiments on co-melt mixtures ranging from 0-100% of each component indicated improved resistance to recrystallization in the glass blends, able to remain fully amorphous for >1 month at 80°C.

■ INTRODUCTION

Luminescent organic materials have attracted significant recent attention due to their role in a variety of functional devices. One particular area of interest comprises organic light emitting diodes (OLEDs), which operate based on charge injection and radiative recombination in multi-layer devices. A related but more specialized application that is based on similar principles of charge transport and exciton mobility involves organic materials for the detection of ionizing radiation. This application serves as the basis for nuclear non-proliferation detection of illicit nuclear materials such as highly enriched uranium or plutonium. By analogy to OLEDs, the performance of an organic scintillator is controlled by the efficiency and kinetics of radiative decay processes that are associated with ion recombination and exciton transport. Another requirement that governs the practical implementation of both applications involves achieving stable optical, electronic, and morphological properties. The ideal scintillator material can be characterized as having:

- 1) minimal optical self-absorption
- 2) fast emission timing (fast counting)
- 3) emission wavelength matching to photodetector (typically 300 to 500 nm)
- 4) high conversion of radiation energy to visible light (light yield)
- 5) discrimination between different types of radiation
- 6) energy resolution/spectroscopy
- 7) amenable to large sizes, low cost, strength, multiple form factors

For these reasons, we describe here our efforts to improve the radiation detection performance and long-term stability of organic-based scintillators via control over the molecular and bulk properties of transparent organic glasses.

Organic scintillators possess the unique ability to discriminate ionization caused by fast neutron recoils on nuclei from that caused by Compton scattering of gamma-rays on electrons, owing to differences in the emission kinetics of the produced light pulses. These differences are evident in the relative fraction of light produced via prompt singlet fluorescence versus delayed triplet-triplet annihilation (TTA). In practice, nuclear recoils from fast neutron interactions produce a greater proportion of delayed luminescence than gamma-rays and can be identified by their characteristic pulse shape. This is due to a phenomenon known as ionization quenching, which leads to a reduction in the relative proportion of prompt fluorescence for neutron versus gamma-ray events.¹ In mixed fluorophore systems, such as plastics and liquids, Förster resonant energy transfer also plays a role. This technique for identifying the type of incident particle is known as pulse-shape discrimination (PSD).

While this pulse-shape discrimination technique is effective in some materials such as *trans*-stilbene single crystals or liquid scintillation mixtures, there are several limitations that preclude their use in critical applications such as radiation portal monitors used at border crossings and ports-of-entry. First, PSD is easily disrupted by the presence of disorder or impurities. This is primarily due to a reliance upon TTA to provide the delayed emission component. TTA is a bimolecular recombination process that requires Dexter electronic interaction between two triplet excited states, the probability of which decreases exponentially as a function of distance. The presence of disorder or impurities decreases the effective triplet exciton lifetime due to a higher density of trapping sites that compete with TTA. Indeed, Arulchakkaravarthi et al. used X-ray rocking curve analysis to correlate degradation in the light yield and PSD with decreased structural order in melt-grown single crystals.² Related work by Carman et al. has shown a sensitive dependence of the PSD upon the

purity and degree of crystallographic perfection in solution-grown *trans*-stilbene.³ Knowledge gained from these studies have led to commercialization of high-quality *trans*-stilbene single crystals, although several limitations remain. Among these are low fracture toughness, high cost, limited size, and highly anisotropic scintillation response.⁴

The combination of these limitations has led to significant interest in non-crystalline organic scintillators based on polymers and organic liquids.¹ Various strategies have been employed to achieve neutron/gamma PSD in these materials, although the obtained scintillation light yields and discrimination performance have been found to be distinctly inferior to single crystals.^{5,6} In this work, we report on a new class of amorphous organic scintillator that exceeds the scintillation performance of *trans*-stilbene while enabling rapid fabrication via a bulk melt-casting procedure.

RESULTS AND DISCUSSION

Iterative Strategy Led to Discovery of Fluorene as Ideal Scintillating Fluorophore

Given the aforementioned challenges of scintillation-grade stilbene, we began a pursuit for novel crystalline scintillators that address these limitations. We postulated that a fluorophore-bearing molecule that crystallizes in a cubic space group could give the desired optical, mechanical, and photophysical properties. Many of these considerations are controlled by second-rank tensors, which are symmetry-dependent properties that include the transport mobility, stress, strain, thermal expansion coefficient, and dielectric constant, among others.⁷ It is known that without bearing some element of symmetry, organic molecules tend to crystallize in lower symmetry space groups (i.e. triclinic or monoclinic), which establishes limitations on these properties.⁸ One relevant example relates to the dissipation of stresses in a low-symmetry crystal such as *trans*-stilbene. In this case, brittle fracture is a typical failure mode due to an insufficient number of independent slip systems to dissipate an applied stress.

In a previous study, it was discovered that compounds **1** and **2** crystallized in higher-order cubic, trigonal, and orthorhombic space groups (Figure 1).⁹ The organization of chromophores in these higher-symmetry arrangements were found to provide improved PSD over crystals of the low-symmetry parent chromophores by virtue of stronger intermolecular triplet energy transfer interactions.¹⁰

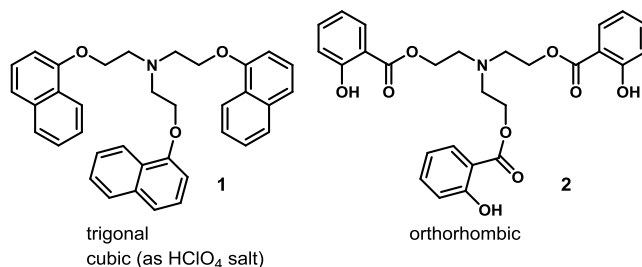


Figure 1. Initial discovery of C_3 -symmetric crystalline scintillators.

In the current work, we synthesized C_3 -symmetric analogs of **1** and **2** to evaluate the relationship between structure and radioluminescence (Figure 2a). Even with the success of compounds **1** and **2**, any modification made to the fluorophore produced materials that had low solubility in common solvents, precluding the ability to grow large crystals. This was the case for typical scintillating fluorophores such as anthracene, 2,5-diphenyloxazole, biphenyl, *p*-terphenyl, *trans*-stilbene, and naphthyl. Substituting the ethyleneoxy-linker for methylene or ethylene improved solubility; however, many of the compounds were not very luminescent, or were prone to slow decomposition. It was hypothesized that electron transfer quenching from the nitrogen lone pair could be in effect. In an attempt to negate any quenching, various amine salts were prepared from the parent molecule, but they were again plagued by low solubility. Substituting silicon for nitrogen brought an improvement in both solubility and luminescence, although not yet to the level required for the present application.

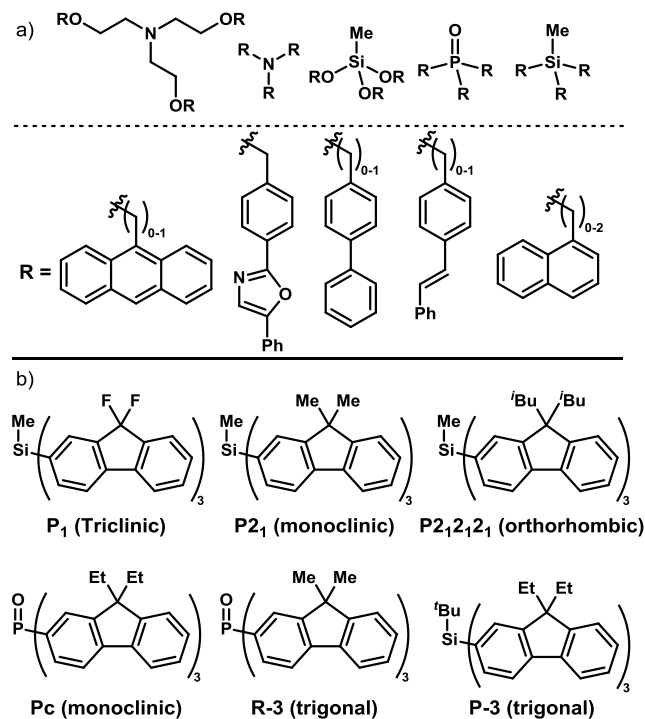


Figure 2. a) Examples of iterative changes to central structure and fluorophore that demonstrated poor radiolumines-

cence and/or poor solubility b) Generation of crystalline compounds demonstrating improved radioluminescence.

Considering that the photophysics of organic light-emitting diode (OLED) emitters are strikingly similar to the principles of radioluminescence in scintillators, we evaluated fluorene as a potential fluorophore group.¹¹ Despite emitting in the 420 nm region, fluorene and its derivatives have not been widely explored in the context of scintillators. Fluorene possesses an advantage in that it can be readily derivatized at the benzylic position to provide oxidative stability and enable facile modification of properties.

We found that compounds based on fluorene chromophores were not only capable of crystallization into higher symmetry space groups (Figure 2b), but also capable of providing higher scintillation light yields and PSD performance than *trans*-stilbene.¹² These properties were evident in initial radiation measurements performed on small crystals (~3 mm), although subsequent measurements on larger crystals revealed somewhat degraded properties due to fluorescence self-absorption.

Organic Glass Scintillators: Improvements with Wavelength Shifters, Limitations with Stability

Singlet wavelength shifters

As is typical for novel material characterization, a melting point analysis was performed on compound **3**, and it was observed that upon cooling the samples remained in a transparent glassy state. This finding provided the opportunity to explore several key objectives: (1) ability to circumvent single-crystal growth procedures as a route towards larger radiation detector elements, (2) ability to improve the photophysical properties via control over secondary dopant concentrations, (3) ability to achieve isotropic optical, mechanical, and transport properties.¹³

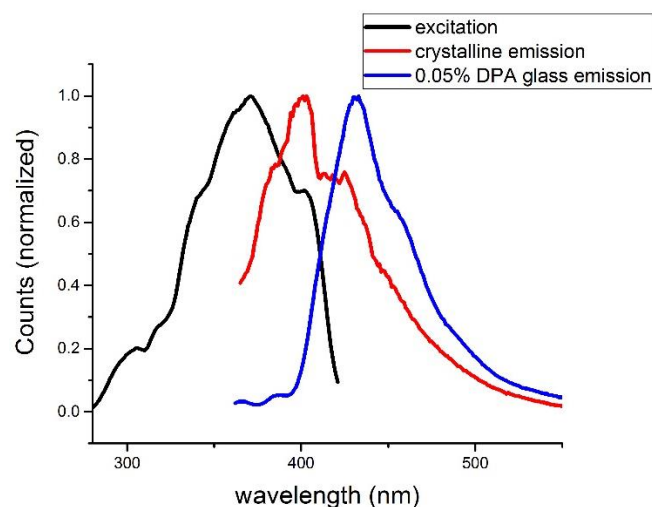


Figure 3. Photoluminescence excitation and emission spectra of **3** in the microcrystalline form (red) and glass with DPA (blue).

Casting amorphous thin films with long term resistance to crystallization is a challenge frequently encountered in the OLED field that directly impacts the lifetime and conditions under which the device can be operated. The observation of a stable glassy state for compound **3** represented a paradigm shift in scintillator research that has related implications for improving OLED device stability and performance. The nature of the glassy state also enables facile tuning of the fluorescence properties. Indeed, by casting a glass of **3** with 0.05% of 9,10-diphenylanthracene (DPA) the Stokes' shift was increased to possess less self-absorption than undoped microcrystalline **3** (Figure 3). With this revelation we no longer constrained ourselves to C_3 -symmetric molecules, but instead focused on structures that could be cast as organic glasses. A review of the literature revealed compound **4** and **5** to possess a glass state as observed by differential scanning calorimetry (DSC).¹⁴ Assessment of the radioluminescence of **4** showed an improvement in the light yield and PSD as compared to **3**. A further improvement in the light yield was made with the incorporation of DPA into the glass. While it was observed that light yield increases in conjunction with DPA concentration, after a threshold concentration the particle discrimination ability diminished (Figure 4). On the 200 mg samples tested, it was determined that the maximum benefit for light yield and PSD was obtained with a DPA concentration of 0.05% (w/w), outperforming stilbene in both respects. A survey of other wavelength shifters emitting in the 400 – 500 nm range demonstrated a similar relationship between performance and concentration, with ca. 0.05% being the optimum concentration (*vide infra*).

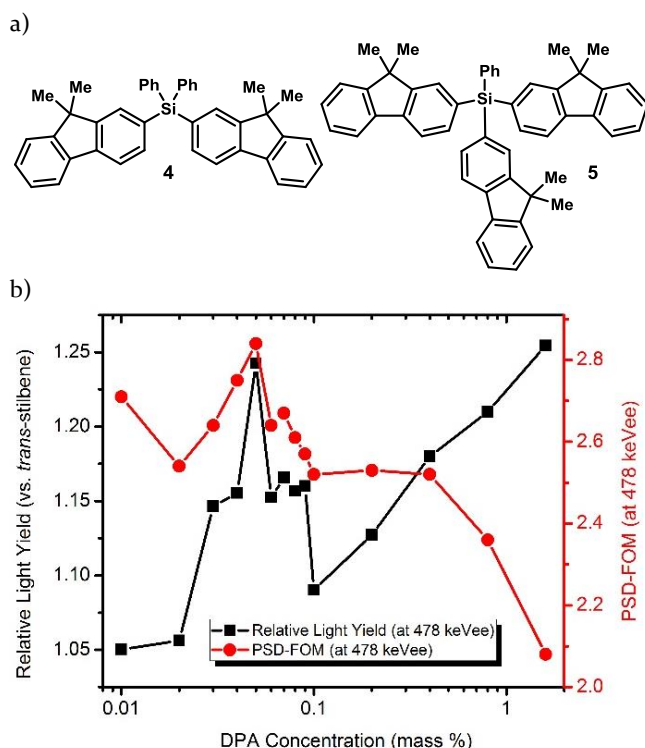


Figure 4. a) Glass forming compounds **4** and **5** b) DPA doping concentration vs light yield and PSD in glass samples of **4**.

Triplet Harvesting Dopants

Taking further inspiration from the OLED literature and similar work in radioluminescent plastics,^{6,15,16} we experimented with the radioluminescence response of glasses containing iridium triplet harvesting dopants. This strategy has been shown to be effective in maximizing the light yield when incorporated in polymer-based host materials at Ir³⁺ concentrations of 0.8-5.5 wt%. Incorporating Bis[2-(4,6-difluorophenyl)pyridinato-C²,N](picolinato) iridium(III) (Flrpic) in organic glass **G1** provided high scintillation light yields at Ir³⁺ concentrations as low as 0.03 wt% (Figure 5). The highest light yields were achieved at 0.13-0.28 wt% Ir³⁺, yielding 1.8-2 times the scintillation light output relative to stilbene. This result indicates efficient triplet harvesting in organic glass matrix **G1**, as reflected by a light yield that is four times greater and an Ir³⁺ doping level six times smaller than for a poly(9-vinylcarbazole) polymer matrix. **Error! Bookmark not defined.** The presence of Ir³⁺ confers a long fluorescence lifetime on the order of 1 μ s, with pulse shapes possessing a very diminished prompt emission peak. The dominance of delayed emission precludes the ability to do particle discrimination; however, the increase in light yield at such a low Ir³⁺ concentration was an interesting discovery in its own right as one of the most sensitive radioluminescent organic materials known.¹

Co-melt Formulation for Indefinite Stability

Comparing scintillators of varying sizes can be challenging due to the fact that some performance variables are size dependent. For example, with overlap of the excitation and emission bands of the glass matrix, re-absorption of the scintillation light can decrease performance as a sample becomes larger, making small samples appear artificially higher performing. Alternatively, small samples have a greater chance of the secondary particle escaping the sample, resulting in incomplete energy deposition and therefore an artificially lower light yield measurement. Due to its higher mass, the secondary proton produced from neutron nuclear recoils will deposit ca. two orders of magnitude more of its energy over a given distance and as a result travel 1/100th the distance as an electron of similar energy and is therefore more likely to completely deposit its energy, even in small samples.¹

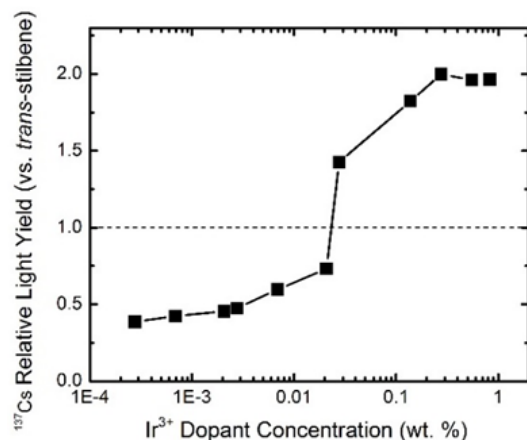


Figure 5. Plot of the relative ¹³⁷Cs scintillation light yield as a function of Ir³⁺ dopant concentration. The glass matrix was a 9:1 mixture of **4:5 (G1)** and the Ir³⁺ complex was Flrpic.

To the best of our knowledge, small-molecule-based organic glasses have never been implemented in large scale applications (ca. > 1 cm³).¹⁷ To make an accurate comparison between our formulation and the state of the art technology, samples had to be prepared on similar sizes to a reference material. To this end, a 2-gram glass sample of **4** was prepared to coincide with the size of benchmark materials on hand. After several weeks at room temperature the sample slowly began to turn opaque on the surface and eventually the entire sample, resulting from crystallization that was confirmed by powder X-ray diffraction (XRD) (Figure 6). Delayed crystallization would make organic glasses ineligible for practical use in the field. The observation of a glass transition temperature (T_g) and lack of solid to liquid transition (T_m) after multiple heating and cooling cycles in a DSC experiment is frequently used to qualitatively assess the stability of a glassy material. It is apparent that this is not true over long durations due to potential kinetic instability of the glassy state.

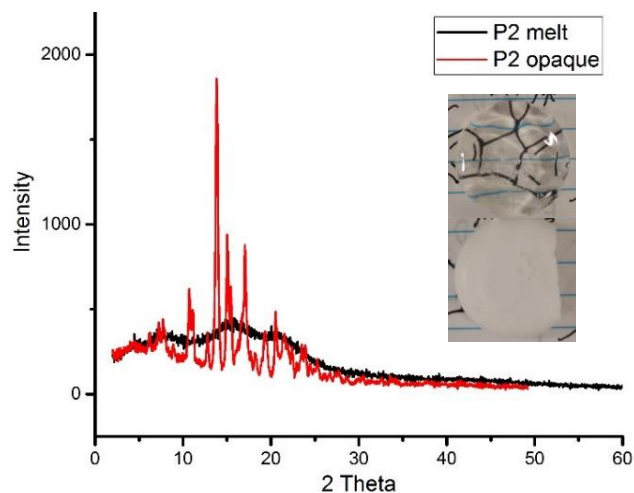


Figure 6. Powder XRD of **4** depicting the change from clear and amorphous 2 gram sample to opaque and crystalline over time.

The glass to crystal transition can proceed by two modes: a glass-to-crystal transition originating from the bulk or originating from the surface.¹⁸ There are known inhibition methods for both types of growth. For example, surface growth can be inhibited by applying a coating,¹⁹ while bulk growth can be inhibited by polymer additives²⁰ or by blending compounds of similar structure.²¹ Increased stability can also be gained when a glass is formed via vapor deposition.²²

At this juncture we instead sought to improve the stability of the glass scintillators via a formulation approach. Since observation of T_g in DSC is not a measure of long term glass stability, each sample was subjected to accelerated aging conditions; whereby, samples were aged at temperatures close to their T_g , a technique known to accelerate crystallization by several orders of magnitude.¹⁴

We found that mixtures of compounds **4** and **5** were indefinitely resistant to crystallization, even under these conditions (Table 1).

Table 1. Co-melt formulation effect on T_g and stability

4 : 5 (w/w) ^a	T_g (°C) ^b	Transparency at 80 °C ^c
100 : 0	72.6	< 24 hours
90 : 10	75.2	> 4 weeks
70 : 30	80.2	> 4 weeks
50 : 50	81.0	> 4 weeks
30 : 70	89.4	> 4 weeks
10 : 90	95.1	< 72 hours
0 : 100	98.9	< 24 hours

^a200 mg samples. ^b T_g value at the onset of the transition. ^cEvaluated by observation using a jeweler's loop.

In a larger scale experiment, a formulation of **4** and **5** demonstrated the same resistance towards crystallization (Figure 7).

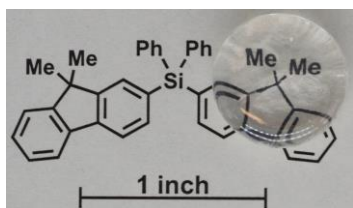


Figure 7. A 2 gram glass sample of **4** and **5** (90:10 w/w) after aging at 60 °C for 72 hours.

Radioluminescence of Organic Glasses: Light Yield, Radiation Timing, PSD, Neutron Response Comparison to Benchmark Materials

Using the best formulation from the wavelength shifter concentration and co-melt studies, we were able to cast 2 gram scintillators containing various dopants (Figure 8) for comparison to benchmark materials of similar dimension (Table 2). Apart from concentration, the identity of the wavelength shifter also had a significant impact of fluorescence and PSD. To our satisfaction, the fluorescence lifetime of singlet emitting doped glasses were faster than stilbene, with the exception of **G2**.

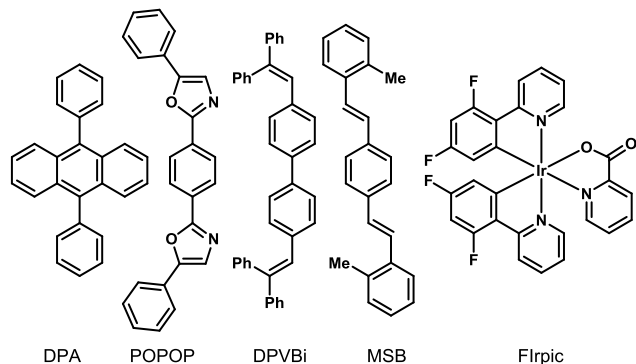


Figure 8. Singlet wavelength shifters and Iridium triplet harvesting dopant.

Table 2. Comparison of radioluminescence of 2 gram glass formulation to known standards

Sample ^a	Dopant (w/w)	Lifetime ^c (ns)	QY ^d (Φ)	Light Yield ^e	PSD ^f
Stilbene ^b	–	2.41	1.00	1.00	3.15
EJ-301	–	2.00 (89%) 16.21 (11%)	0.81	0.63	2.57
EJ-200	–	1.50	0.95	0.63	0.66
G1	–	1.68	1.05	0.62	2.48
G2	0.05% DPA	8.09	0.74	1.11	2.53
G3	0.05% POPOP	1.52	0.92	1.11	3.56
G4	0.05% DPVBi	1.50	1.79	0.88	3.06
G5	0.05% MSB	1.45	1.50	1.10	3.73
G6	0.07% MSB	1.53	1.61	1.14	3.56
G7^g	1% Flrpic	1.01 μs	0.40	2.00	N/A

^aGlass samples composed of 9:1 mixture of **4:5** ^bSingle Crystal of similar size ^cFluorescence lifetime measured at emission maximum ^dRelative to stilbene, measured at the absorption maximum ^eCs-137 relative light yield (478 keVee) ^fPSD-FOM at 478 keVee) ^g200 mg sample.

From this data, **G5** was identified as possessing the best performance with 10% greater light yield and 18% greater PSD. Further analysis of a histogram plot of the data after pulse-processing revealed some interesting features (Figure 9a, b). Similar to stilbene, there is excellent separation between the neutron and gamma bands down to low energy events, a desirable feature not present in organic liquids and plastics. When the binned histogram data is analyzed using the FOM definition and plotted as a function of energy, it is clear that the PSD capability of **G5** outperforms stilbene across the energy range (Figure 9c).

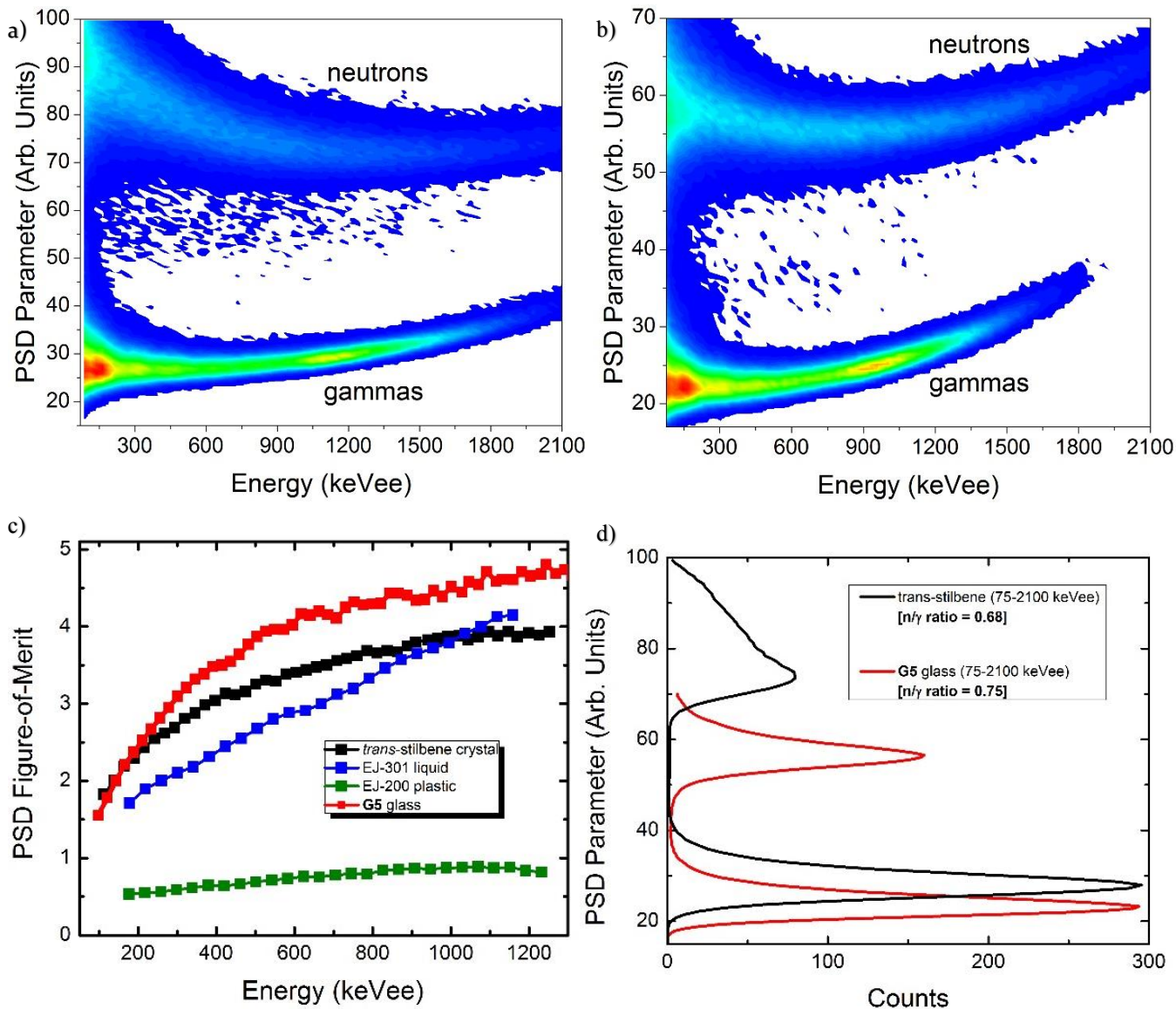


Figure 9. PSD histograms for a) *trans*-stilbene crystal and b) G5 glass obtained using an AmBe mixed n/ γ -ray source. c) Plot of the neutron/gamma pulse-shape discrimination figure-of-merit as a function of gamma-ray energy for G5 glass (red) in comparison to three reference scintillators. d) Total integral of neutron and gamma-ray counts in the energy range of 75-2100 keVee for *trans*-stilbene crystal (black) and G5 glass (red).

Another often overlooked aspect of scintillator performance is the neutron light yield. Since it is difficult to subject samples to a calibrated *neutron* energy source, a *gamma* calibrated PSD plot is typically reported using gamma-ray sources of known energies (i.e. keVee scale units). Often times a scintillator can be formulated to possess a higher PSD-FOM, but at the expense of the neutron sensitivity and light yield. To evaluate neutron sensitivity without utilizing a calibrated neutron source, we simply integrated the counts from the histogrammed data across the relevant energy region with respect to the PSD parameter for G5 and compared it to stilbene under identical conditions (Figure 9d). The larger neutron:gamma integral for G5 reveals that the high PSD-FOM values for G5 does not come at the expense of neutron sensitivity/light yield; in fact, the neutron sensitivity/light yield is higher than stilbene. Since fast neutrons have the highest interaction cross-section with hydrogen atoms, the neu-

tron response is dependent on the hydrogen content of a scintillator. The identical H/C ratios (0.857) for both G5 and stilbene indicate that the improvement in neutron scintillation efficiency is attributed to the scintillation properties and not due to a difference in molecular formula.

Fast scintillation timing is also important for a number of radiation detection applications including correlated particle counting and imaging.²³ To demonstrate that the faster fluorescence timing of G5 was duplicated in the scintillation response, a time correlated single-photon counting experiment was used to construct pulse shapes under ¹³⁷Cs gamma irradiation (Figure 10). As compared to stilbene and EJ-200 reference materials, the glass samples possess faster scintillation rise-time and decay characteristics. This is promising for applications such as active interrogation that demand fast counting as well as neutron discrimination.²⁴

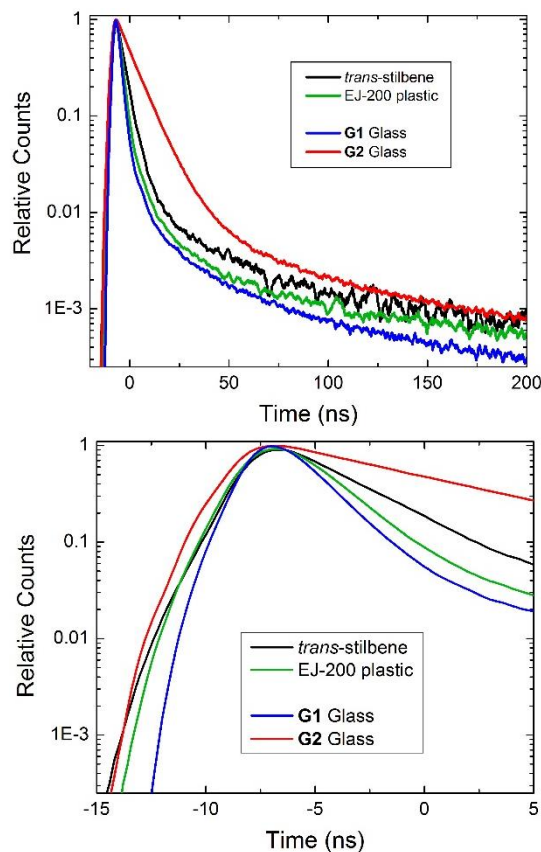


Figure 10. Normalized scintillation timing via time correlated single-photon counting in the presence of a ^{137}Cs source (top), zoomed in region at the pulse max amplitude (bottom).

Scale up and Practical Application

To demonstrate scalability, a casting of **G1** was made in a size and shape that is compatible with many photomultiplier tubes. The resulting sample possessed very good optical transparency and incurred no damage while handling (Figure 11).

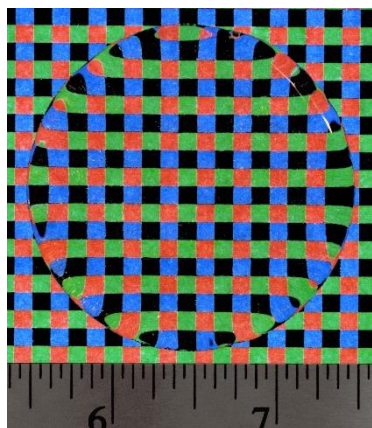


Figure 11. A 2" diameter, $\frac{1}{2}$ " thick casting of **G1** (19 grams).

This observation was encouraging in that practical radiation detection with these materials are possible as a re-

placement for stilbene. There is also the potential of casting into form factors for applications that are not yet realized.

■ MATERIALS AND METHODS

For the reported light yield measurements, the integral of the baseline subtracted pulse from 10 nanoseconds ahead to 170 nanoseconds after the waveform maximum was used as a proxy for total energy deposited. The waveform maximum was determined as the time during the record at which the derivative of the waveform crossed zero; with linear interpolation to provide subsample resolution.

The conversion from this pulse energy to electron equivalent energy (in keVee) was approximated by finding the pulse energy at which the Compton edge reached 70% of the Compton peak value for a ^{137}Cs gamma source measurement.²⁵ We then used 478 keVee/this pulse energy value as a linear conversion to the energy scale.

The pulse shape discrimination parameter used in this work is defined as the time between 10% and 90% of the baseline subtracted pulse integral over the entire waveform record; with linear interpolation to provide subsample resolution. We found that the use of this PSD parameter eliminates the systematic biases that can be introduced by implementing methods that require knowledge of or optimization for the scintillator pulse shape. Because we are comparing multiple scintillating materials with varying pulse shapes, we did not use more popular methods such as the tail to total ratio so as to not bias their relative performance by any particular time window choice.

In order to characterize the PSD performance of each scintillator, we developed a procedure by which an energy dependent Figure of Merit (FOM) is derived. In this work, we use the familiar FOM definition:

$$FOM(E) = \frac{\mu_n(E) - \mu_\gamma(E)}{(\Gamma_n(E) + \Gamma_\gamma(E))}$$

Where μ stands for the mean of a distribution, Γ stand for the full width at half maximum (FWHM) of a distribution, and the subscripts n and γ refer to the neutron and gamma distributions respectively.

■ CONCLUSION

The current work is the first example of organic glasses as a new class of materials for radiation detection. The development of a high quantum yield matrix in an easily processable form factor is the next evolutionary step in the field of radiation detection and discrimination. The ease by which additives can be incorporated into the matrix imparts versatility in designing new types of scintillators. As compared to benchmark materials, improvements were made across all metrics we measured, including light yield, pulse-shape discrimination, neutron response and timing. The combination of these improvements can lead to radiation detectors with better detection efficiency, which enhance our national security and non-proliferation mission capabilities.

To the best of our knowledge, this is also the first example of a large (> 1 gram), indefinitely stable small-molecule organic glass, which was achieved through formulation of two different scintillating compounds. This stable formulation provides a platform for many possibilities, including further development of high Z-doped glasses for gamma spectroscopy.

ASSOCIATED CONTENT

The Supporting Information is available free of charge on the ACS Publication website at DOI: ###, which includes: experimental procedures for the synthesis and casting of glasses, photoluminescence spectra, radioluminescence data, DSC spectra and X-ray crystallographic data.

AUTHOR INFORMATION

Corresponding Author

*plfeng@sandia.gov

Author Contributions

The manuscript was written through contributions of all authors.

Funding Sources

This work was supported by the office of NA-22, NNSA, U.S. Department of Energy. Sandia National Laboratories is a multi-mission laboratory managed and operated by National Technology and Engineering Solutions of Sandia, LLC., a wholly owned subsidiary of Honeywell International, Inc., for the U.S. Department of Energy's National Nuclear Security Administration under contract DE-NA0003525.

Notes

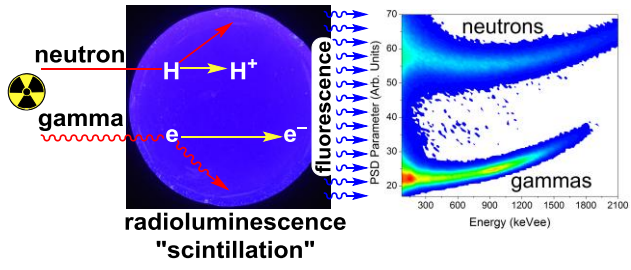
The authors declare no competing financial interest.

ACKNOWLEDGMENT

We would like to thank F. Patrick Doty and Mateusz Monterial for lively discussions.

REFERENCES

- (1) Knoll, G. F. *Radiation Detection and Measurement*, 4th ed.; John Wiley & Sons: Hoboken, NJ, 2010.
- (2) Arulchakkaravarthi, A.; Balamurugan, N.; Kumar, R.; Santhanaraghavan, P.; Muralithar, S.; Nagarajan, T.; Ramasamy, P. *Mat. Lett.* **2004**, *58*, 1209–1211.
- (3) Carman, L.; Zaitseva, N.; Martinez, H. P.; Rupert, B.; Pawelczak, I.; Glenn, A.; Mulcahy, H.; Leif, R.; Lewis, K.; Payne, S. *J. Cryst. Growth* **2013**, *368*, 56–61.
- (4) Schuster, P. F. Investigating the Anisotropic Scintillation Response in Organic Crystal Scintillator Detectors. Ph.D. Dissertation, UC Berkeley, Berkeley, CA, 2016.
- (5) Bourne, M. M.; Clarke, S. D.; Adamowicz, N.; Pozzi, S. A.; Zaitseva, N.; Carman, L. *Nucl. Instrum. Methods Phys. Res., Sect. A* **2016**, *806*, 348–355.
- (6) Feng, P. L.; Villone, J.; Hattar, K.; Mrowka, S.; Wong, B. M.; Allendorf, M. D.; Doty, F. P. *IEEE Trans. Nucl. Sci.* **2012**, *59*, 3312–3319.
- (7) Prakash, O.; Jones, D. R. H. *Acta. Metall. Mater.* **1992**, *40*, 3443–3449.
- (8) Price, S. L. *Chem. Soc. Rev.* **2014**, *43*, 2098–2111.
- (9) a) Pramanik, A.; Bhuyan, M.; Choudhury, R.; Das, G. *J. Mol. Struct.* **2008**, *879*, 88–95. b) Jiang, L.-J.; Pan, Z.-Q.; Duan, C.-Y.; Luo, Q.-H.; Liu, Y.-J.; Huang, X.-Y.; Wu, Q.-J. *J. Chem. Crystallogr.* **1999**, *29*, 943–947.
- (10) Feng, P. L.; Foster, M. E. *IEEE Trans. Nucl. Sci.* **2013**, *60*, 3142–3149.
- (11) For a review of light-emitting diodes structure and function see a) Shirota, Y.; Kageyama, H. *Chem. Rev.* **2007**, *107*, 953–1010. b) Walzer, K.; Maennig, B.; Pfeiffer, M.; Leo, K. *Chem. Rev.* **2007**, *107*, 1233–1271. c) Jou, J.-H.; Kumar, S.; Agrawal, A.; Li, T.-H.; Sahoo, S. *J. Mater. Chem. C* **2015**, *3*, 2974–3002.
- (12) Carlson, J. S.; Feng, P. L. *Nucl. Instrum. Methods Phys. Res., Sect. A* **2016**, *832*, 152–157.
- (13) With limited exceptions: a) Dawson, K. J.; Zhu, L.; Yu, L.; Ediger, M. D. *J. Phys. Chem.* **2011**, *115*, 455–463. b) Eich, M.; Looser, H.; Yoon, D. Y.; Twieg, R.; Bjorklund, G.; Baumert, J. C. *J. Opt. Soc. Am. B* **1989**, *6*, 1590–1597.
- (14) Wei, W.; Djurovich, P. I.; Thompson, M. E. *Chem. Mater.* **2010**, *22*, 1724–1731.
- (15) Campbell, I. H.; Crone, B. K. *Appl. Phys. Lett.* **2007**, *90*, 012117-1–3.
- (16) Rupert, B.L.; Cherepy, N.J.; Sturm, B.W.; Sanner, R.D.; Payne, S.A. *Europhys. Lett.* **2012**, *97*, 22002-1–4.
- (17) a) Shirota, Y. *J. Mater. Chem.* **2000**, *10*, 1–25. b) Molaire, M. F.; Johnson, R. W. *J. Polym. Sci., Part A: Polym. Chem.* **1989**, *27*, 2569–2592. c) Koop, T.; Bookhold, J.; Shiraiwa, M.; Pöschl, U. *Phys. Chem. Chem. Phys.* **2011**, *13*, 19238–19255.
- (18) a) Xi, H.; Sun, Y.; Yu, L. *J. Chem. Phys.* **2009**, *130*, 094508-1–9. b) Cai, T.; Zhu, L.; Yu, L. *Pharm. Res.* **2011**, *28*, 2458–2466.
- (19) Wu, T.; Sun, Y.; Li, N.; de Villiers, M. M.; Yu, L. *Langmuir* **2007**, *23*, 5148–5153.
- (20) Powell, C. T.; Chen, Y.; Yu, L. *J. Non-Cryst. Solids* **2015**, *429*, 122–128.
- (21) Wu, Y.-C. M.; Molaire, M. F.; Weiss, D. S.; Angel, F. A.; DeBlase, C. R.; Fors, B. P. *J. Org. Chem.* **2015**, *80*, 12740–12745.
- (22) Swallen, S. F.; Kearns, K. L.; Mapes, M. K.; Kim, Y. S.; McMahan, R. J.; Ediger, M. D.; Wu, T.; Yu, L.; Satija, S. *Science* **2007**, *315*, 353–356.
- (23) a) Goldsmith, J. E. M.; Gerling, M. D.; Brennan, J. S. *Rev. Sci. Instrum.* **2016**, *87*, 083307. b) Monterial, M.; Marleau, P.; Pozzi, S. A. *IEEE Trans. Nucl. Sci.* **2017**, *in press*, DOI: 10.1109/TNS.2017.2647952.
- (24) Runkle, R. C.; Chichester, D. L.; Thompson, S. J. *Nucl. Instrum. Methods Phys. Res., Sect. A* **2012**, *663*, 75–95.
- (25) The approximation of the Compton edge at 70% of the peak is a close approximation of the correct energy scale, and typical for organic scintillators: Dietze, G.; Klein, H. *Nucl. Instrum. Methods* **1982**, *193*, 549–556.



For Table of Contents Only